Spatially selective RF quadratic fields excitation

Yi-Cheng Hsu[1], I-Liang Chern[1], and Fa-Hsuan Lin[2,3]
[1]National Taiwan University, Taipei, Taiwan, [2]National Taiwan University, Taiwan, [3]Massachusetts General Hospital, United States

INTRODUCTION

MRI of a small FOV with limited scanning time can have image aliasing artifact. In high field MRI, as the FOV approximates the wavelength of the RF signal transmission/reception, wave interferences can cause deleterious inhomogeneous flip angle distribution (a larger $|B_1^+|$ in the center of a volume coil and a smaller $|B_1^+|$ in the periphery of a volume coil) [1]. Both challenges can be mitigated by designing spatially selective RF excitation, which has been commonly implemented in MRI scanners with a longer pulse duration using linear gradient fields. Spatially selective RF excitation can be completed faster when parallel RF transmission, such as RF shimming [2, 3] and transmit SENSE [4], is used.

Recently, using nonlinear spatial magnetic fields in MRI signal encoding has been demonstrated to improve MRI spatiotemporal resolution [5, 6]. Preliminary studies using hyperbolic paraboloids (saddle shape) nonlinear gradient for RF excitation [7] and small FOV imaging [8] have also been reported. Here we propose using the combination of magnetic fields with linear and paraboloid of revolution (bowel shape) fields to efficiently achieve spatially selective RF excitation ***without*** parallel RF transmission. In particular, we demonstrate this quadratic field excitation (QFE) in 1) small FOV imaging and 2) generating a spatial profile to compensate spatially inhomogeneous $|B_1^+|$ with a *single* RF transmitter. For small FOV imaging, QFE is more than two times faster and can improve the accuracy of the excitation profile by 2.2-fold without using a later slice selective 180° refocusing pulse. For B1 inhomogeneity improvement, QFE is 2.5 times faster than fast-K_z [9], to excite a slice with in-plane circular symmetric flip angle distribution (smaller/larger flip angle at central/periphery of FOV) with more extreme flip angles.

METHODS

Taking the small-tip angle approximation, the dynamics of complex-valued transverse magnetization $M_{xy}(\mathbf{r},t)=M_x(\mathbf{r},t)+jM_y(\mathbf{r},t)$ at location **r** in the rotation frame neglecting T_1 and T_2 relaxation can be described by the Bloch equation: $dM_{xy}(\mathbf{r},t)/dt = -j\gamma\langle\mathbf{g}(t)\bullet\mathbf{f}(\mathbf{r})\rangle M_{xy}(\mathbf{r},t)+j\gamma B_1(t)M_0$, where M_0 is the z-component of the magnetization, $B_1(t)=B_{1x}(t)+jB_{1y}(t)$ describes the instantaneous RF excitation field, $\mathbf{g}(t)$ denotes the instantaneous gradient fields for spatial encoding, and γ is the gyromagnetic ratio [10]. $\mathbf{f}(\mathbf{r})$ describes the spatial distribution of the z-directional component linear or nonlinear spatial encoding magnetic fields SEMs). Traditionally $\mathbf{f}(\mathbf{r})=\mathbf{r}$. By the end of RF excitation at T, the transverse magnetization is an inverse Fourier transform:

$$M_{xy}(\mathbf{f}(\mathbf{r})) = j\gamma M_0 \int_K W(\mathbf{k})\exp[j2\pi\langle\mathbf{f}(\mathbf{r})\bullet\mathbf{k}\rangle]s(\mathbf{k})d\mathbf{k},\ \mathbf{k}(t)=\frac{\gamma}{2\pi}\int_t^T \mathbf{g}(s)ds$$

, where $s(\mathbf{k})$ describes a trajectory using delta functions in *k*-space, $W(\mathbf{k})=B_1(t)/|\mathbf{k}'(t)|$, $\mathbf{k}'(t)=d\mathbf{k}(t)/dt$. When *n* distinct SEMs are used for RF excitation, $\mathbf{f}(\mathbf{r})$ maps between the *m*-dimensional real space coordinates (x,y,z; m=3) and the *n*-dimensional encoding space coordinates ($f_1,f_2,\ldots f_n$, where f_i denotes the i^{th} SEM). Importantly, if the target magnetization profile $M_{xy}(\mathbf{r})$ can be described by $M_{xy}(\mathbf{f}(\mathbf{r}))$, then the encoding dimension can be changed from *m*-dimensional to *n*-dimensional *k*-space (potentially $n<m$) for more efficient encoding.

Here we use two SEMs (linear Z gradient, $f_1(\mathbf{r}) = f(z) = z$, and a nonlinear Z2 gradient, $f_2(\mathbf{r}) = f(x,y,z) = z^2 - 1/2(x^2+y^2)$; n=2) to demonstrate the advantage of QFE. The first example is small FOV excitation in 3D. Specifically, we aim at exciting a circular planar ROI with the width = 1/3 FOV. The second example is to excite a single slice with the distribution of the strength of M_{xy} as a constant minus a 2D Gaussian in order to reduce inhomogeneous RF excitation in high field MRI. We used σ^2 the ratio between the L2 norm of the difference between ideal and excited profiles and the power of the ideal profile to quantify the accuracy of the excitation.

QFE was also applied to generate a distribution of $|M_{xy}|$, which has smaller and larger magnitudes at the center and periphery of the FOV respectively. This application aims to reduce the high field $|B_1^+|$ inhomogeneity when a volume coil is used for RF excitation. For comparison, we implemented the Fast-kz method using 5 spokes.

RESULTS

Figure 1 shows the ideal profile of M_x in an experiment aiming at excite the central 1/3 FOV excited by 25 spokes using traditional linear gradients as well as QFE using 25 and 11 spokes using Z2 and Z linear gradients. When both QFE and linear gradient both use 25 spokes, σ^2 was improved from 44% to 14%. Taking the time to excite 25 spokes as the 100% relative time (T_{rel}), QFE 11 spokes spent only 44% of time and achieves better profile (σ^2=20%) than the result using linear gradients and 25 spokes (σ^2=44%).

Fig.1

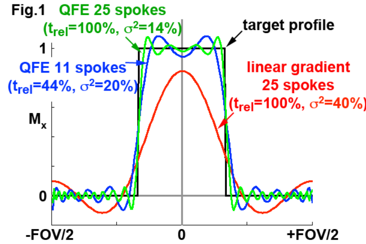

Fig. 2

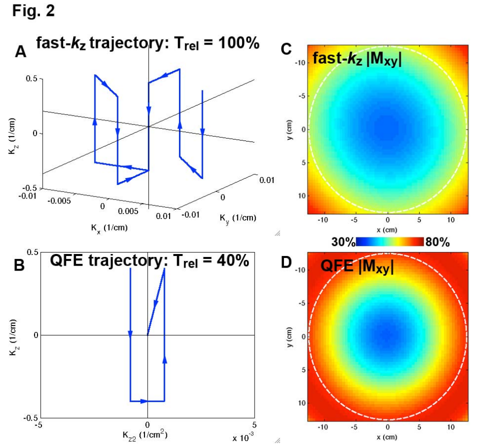

Figure 2 show the *k*-space trajectories of QFE and Fast-K_z (A and B) and the associated distribution of $|M_{xy}|$ (C and D). Note that QFE can generate the desired $|M_{xy}|$ distribution (smaller/larger $|M_{xy}|$ at central/periphery of the FOV) with more extreme values than Fast-K_z: (QFE: max/min=0.73/0.39; Fast-Kz: max/min=0.60/0.40). Importantly, this 2-spoke is 2.5-fold faster than 5-spoke Fast-K_z for the desired excitation pattern.

DISCUSSION

We demonstrate quadratic field excitation (QFE) using one single RF transmitter to generate efficient small FOV magnetization excitation and a complementary $|M_{xy}|$ distribution to mitigate the $|B_1^+|$ inhomogeneity challenge in high field MRI. Similar to small FOV excitation using linear gradients, the limit of QFE in small FOV imaging depends on the trade-off between the allowed excitation time and the sharpness/width of the FOV. Practically, the duration of QFE depends on the slew rate of the Z2 gradient. However, since the Z2 gradient only moves the spokes along Kz2, we expect that the time spent on traversing this part of the QFE trajectory is marginal.

QFE can generate not only true circularly symmetric magnetization distribution, but also rotated elliptical distributions when the full linear and quadratic fields are used, to reduce high field $|B_1^+|$ inhomogeneity. Importantly, QFE does not need parallel RF transmitter and thus avoid the technical challenge of accurate B_1^+ mapping for each transmitter [11].

REFERENCES

1. Vaughan, J.T., et al., Magn Reson Med, 2001. **46**(1): p. 24-30.
2. Mao, W., M.B. Smith, and C.M. Collins, Magn Reson Med, 2006. **56**(4): p. 918-22.
3. Collins, C.M., et al., Magn Reson Med, 2005. **54**(6): p. 1327-32.
4. Katscher, U., et al. Magn Reson Med, 2003. **49**(1): p. 144-150.
5. Stockmann, J.P., et al., Magn Reson Med, 2010. **64**(2): p. 447-56.
6. Hennig, J., et al., MAGMA, 2008. **21**(1-2): p. 5-14.
7. Weber, H., et al., Proc. Intl. Soc. Magn. Reson. Med., 2011: p. 2806.
8. Witschey, W.R., et al., Proc. Intl. Soc. Magn. Reson. Med., 2011
9. Saekho, S., et al., Magn Reson Med, 2006. **55**(4): p. 719-24.
10. Pauly, J.M., D.G. Nishimura, and A. Macovski, J Magn Reson, 1989. **81**: p. 43-56.
11. Setsompop, K., et al., Magn Reson Med, 2006. **56**(5): p. 1163-7